Theoretical Performance Analysis of Fixed Pitch Propeller Operating at Low Reynolds Number Conditions

Milan Adhikari [a], Hari Dura [b], Laxman Poudel [c], Lokesh Silwal [d]

[a, b, c] *Department of Mechanical Engineering, Pulchowk Campus, IOE, TU, Nepal*
[d] *Department of Aerospace Engineering, Auburn University, USA*
Corresponding Email: [a] 074msmde008.milan@pcampus.edu.np, [b] duraharis@pcampus.edu.np,
[c] p12_laxman@yahoo.com, [d] lzs0082@auburn.edu

Abstract

The propeller performance data at its design point and off design points are the basis for the selection of suitable propeller for an unmanned air vehicles (UAVs) system. Various research have been conducted for the development of a low-fidelity tool for theoretical prediction of the propeller performance but are not readily available in the public domain. In addition, the commercially available propellers only have performances at on-design points. Thus, the current work focuses on developing an analytical tool for the prediction of the propeller performance which is based on the Blade Element Momentum Theory (BEMT). The traditional BEMT theory has been adapted and modified to include the effects of radial variations in the blade and flow properties for increasing the accuracy of prediction. The airfoil properties at various radial sections have been calculated from the XFOIL data base and the tool has been developed in Matrix Laboratory (MATLAB). An arbitrary base line propeller has been chosen for developing the current tool. The preliminary calculations were carried out at the rotating speed and free stream velocity of 7500 RPM and 80 m/s respectively. The efficacy of the prediction tool were then explored at various on-design operating conditions. The rotating speed and forward speed were changed from 6500 RPM to 8500 RPM and from 65 m/s to 90 m/s respectively. The performance analysis was done for the designed base line propeller to study the effects of rotational speed and free-stream velocity. For the base line propeller at its design point, the thrust coefficient, torque coefficient and propulsive efficiency were calculated to be 0.0724, 0.0347 and 83.5% respectively.

Keywords

Propeller, BEMT–XFOIL

1. Introduction

Application of UAVs is increasing in various fields such as search and rescue operation, agricultural, atmospheric research, surveying and medical delivery worldwide. The number of research pertaining to the design, performance and navigation of the drones has increased drastically over the recent years. In context of Nepal, there is a recent surge in the interest in UAVs and drones with applications extending from civil to military sectors. But the amount of research carried out in Nepal in this field has been limited. One of the recent study carried out in Nepal focused on developing a baseline guidance for navigation and control system for medical delivery UAVs [1]. There is a need for increased number of similar research in the field of drones with applications specific to the topology of Nepalese terrains. Thus, this project is aimed at making a small contribution to the growing field of UAVs and drones by developing a low-fidelity tool that can easily be adapted by the end-user to make vital operating decisions.

As a first step, we are focusing on developing a model for an accurate prediction of a single, two-bladed propellers. Propellers are the commonly used source of propulsion for the UAVs system which creates thrust in same direction as the axis of rotation. Propeller acts like a rotating wings and creates pressure difference between its upper and lower surfaces. The overall performance of an UAVs system can be analysed by analyzing on design and off design performance of its propellers. For a propeller, its free stream velocity (V_∞), rotational speed (W) along with air density (ρ) and viscosity (ν) define the operating condition. Performance of a propeller is analysed

using number of performance parameters such as advanced ratio(J), thrust coefficient (C_T), torque coefficient (C_Q), propulsive efficiency (η). There exits number of analytical methods to calculate the performance parameters of a propeller which includes momentum theories, blade element theories, combined blade element theories and lifting line theories [2]. The current study uses the combined blade element momentum theory (BEMT). Figure 1 shows a cross-section of a propeller with velocity triangle and the forces acting on it.
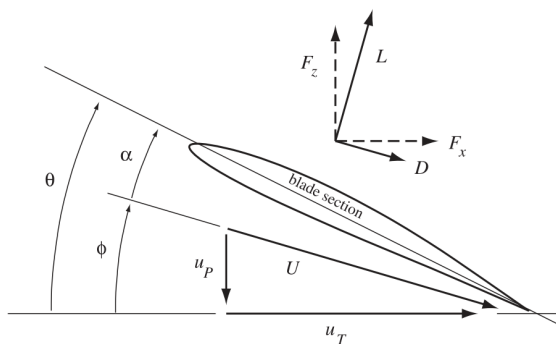

Figure 1: Velocity Triangle and Forces in a Propeller Section [2]

Blade element theory combines the basic principles from both blade element and momentum approaches. BEMT analysis of propeller discretizes the blade into number of sections in radial direction. Then each element is considered as a 2D lifting element, by neglecting the spanwise effects. The sectional thrust and torque can be found by applying force balance to the blade element in both axial and circumferential directions. Finally the total thrust and torque value of propeller are calculated by integrating the the sectional values in the spanwise direction. The mathematical details of the BEMT theory has been discussed in the Methodology section below.

1.1 Problem Statement

The availability of the propeller performance data at the design point and off design points is the basis for the successful design of UAVs system. The performance data that are easily available and catalogued systematically are mostly for the larger propeller with diameter 4 feet and more, which operates at high Reynolds number [3]. Because of the smaller chord length, the propeller used for small UAVs operates in low Reynolds number. There is not sufficient performance data for propeller operates in

low Reynolds number [4]. Various researches have been conducted to develop a tool for the prediction of propeller performance using BEMT but are not available in public domain [5][6]. The performance of propeller varies according to its operating conditions because of the resultant Reynolds number and air density. But the manufacturer of commercially available propeller provides the propeller performance at its design point only which is not sufficient for the selection of propeller for specific operating conditions. Thus, the main motive of this research work is to develop a low fidelity propeller performance prediction tool based on BEMT using MATLAB programming language.

1.2 Scope and Limitation

Most of the commercially available propeller are designed with two blades and fixed pitch. So the study is limited to the performance analysis of fixed pitch propeller with two blades. The aerodynamics data for airfoil will be generated using XFOIL. Previous research shows that the output of XFOIL shows good agreement with experimental and CFD analysis within stall regions [7][8].This research is limited to the study of propeller performance with in an operational bounds which will constrain the angle of
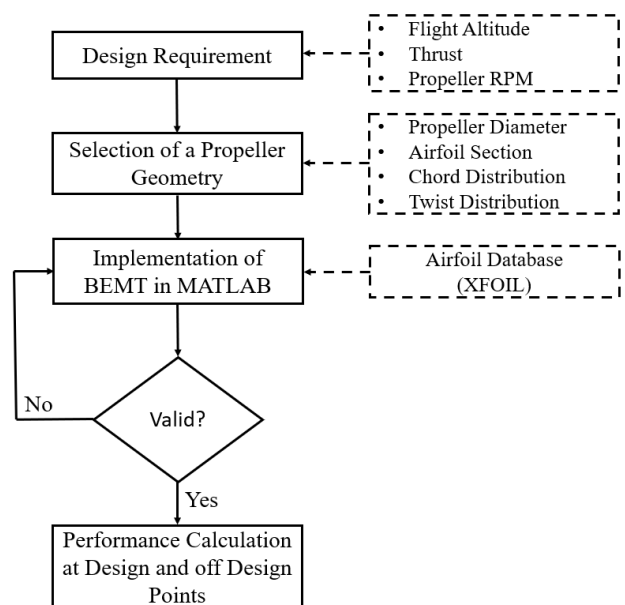
2. Methodology

Figure 2: Research Methodology Flowchart

For the baseline propeller, the design parameters such as flight altitude, output thrust and RPM were defined at its design point. A propeller geometry was selected

by defining diameter, airfoil, radial distribution of chord and geometric angle. Operating condition was defined and the range of sectional Reynolds number and angle of attack were calculated. Three dimensional database of airfoil aerodynamic properties was created in MATLAB using XFOIL. BEMT algorithm was implemented in MATLAB to develop a theoretical performance prediction tool. The output from tool was compared with Harrington Rotor1 full scale experimental data to validate the tool. The performance parameters such as thrust coefficient, torque coefficient and propulsive efficiency were predicted for base line propeller. Flowchart for the methodology is presented in figure 2.

2.1 Base line Propeller Design

2.1.1 Operating Condition

The propeller is to be designed for high altitude application. The operating elevation of propeller was set to be 4000 m from sea level and the values of density and viscosity at this elevation were obtained from Norman et. al [9]. For design point, the rotational speed was set to 7500 RPM . Forward speed of propeller at its design point was set to 80 m/s based on its application. Table 1 summarizes the operating condition of designed propeller.

Table 1: Operating Conditions of Propeller

Parameters	Minimum	Maximum
Rotational Speed, RPM	6500	8500
Forward Speed, m/s	65 m/s	90 m/s

2.1.2 Geometric Angle Distribution

The diameter of propeller was taken as 10 inch i.e 0.254 m and for the simplicity a single airfoil section NACA 2412 was selected as the sectional airfoil. Maximum efficiency of propeller will be obtained if all the airfoil sections along the blade span are at their maximum efficient angle of attack. For basic design of propeller, the local Reynolds number for each section of blade was set to be 50,000, which was the local Reynolds number value for the mid-span of the blade.

From the aerodynamics database, the most efficient angle of attack for selected airfoil at Reynolds number value 50,000 was found to be 5 degree. Based on this, from the velocity triangle of each section the
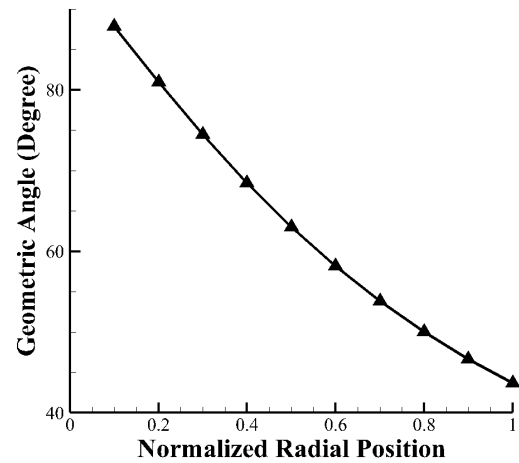

Figure 3: Radial Distribution of Geometric Angle

geometric angle for different normalized radial position was calculated by adding the desired operating angle of attack i.e. 5 degree with the local inflow angle calculated from the operating rotational and forward velocity at design point. Figure 3 shows the obtained radial distribution of the geometric angle.

2.1.3 Chord Distribution

The chord distribution of propeller airfoil section with respect to its radial position was calculated based on the relation below provide by Liu et. al [10].

$$c = (0.084241 - 0.85789r + 4.7176r^2 - 9.6225r^3 + 8.5000r^4 - 2.7959r^5)D \tag{1}$$

Where c is the local chord length, r is the normalized radial position and D is the diameter of propeller. Figure 4 shows the radial distribution chord length for designed propeller.
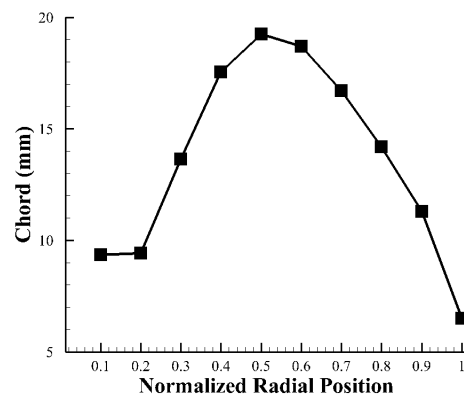

Figure 4: Radial Distribution of Chord Length

2.2 Airfoil Aerodynamic Database

For designed propeller operated in its operational bound, it was found that the sectional Reynolds number varies from 20000 to 110000. An aerodynamic database which contains the variation of lift and drag coefficient with respect to angle of attack was created using XFOIL for the operating range of Reynolds number. A three dimensional matrix was created with angle of attack, lift and drag coefficient and Reynolds number as the variables. Figure 5 and figure 6 show the representative aerofoil aerodynamic database for Re 20,000, 45,000 and 75,000 for NACA 2412 airfoil section.
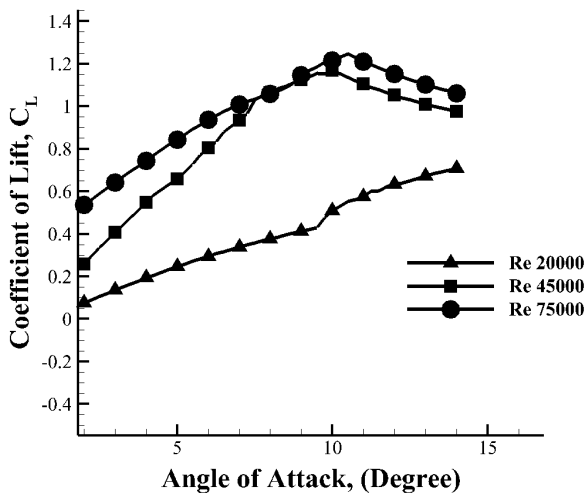

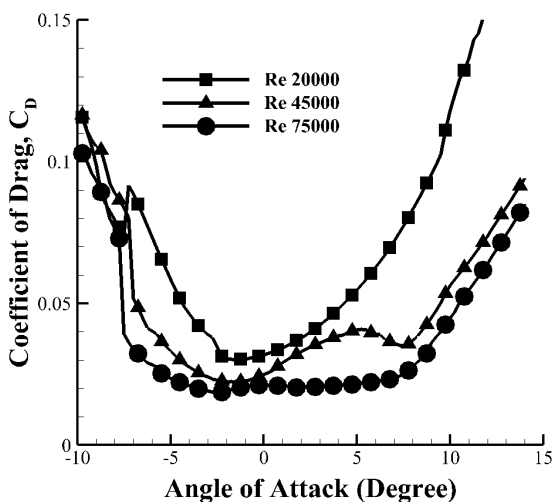
Figure 5: Angle of Attack vs Lift Coefficient

Figure 6: Angle of Attack vs Drag Coefficient

It was observed that the airfoil stalled at angles close to

10° for larger Reynolds number of 45,000 and 75,000. For smaller Reynolds number of 20,000, the linear range for the airfoil was observed to be below 10°. The plot for the drag coefficient (Figure 6) is also in part with the lift coefficient plot as sudden increase in drag after the stall angle was observed.

2.3 Propeller Performance Parameters and BEMT

Mathematical expression for various parameters which are associated with the analysis of propeller are listed below.

$$C_T = \frac{T}{\rho n^2 D^4} \qquad (2)$$

$$C_Q = \frac{Q}{\rho n^2 D^5} \qquad (3)$$

$$\eta = \frac{1}{2\pi} \frac{C_T}{C_Q} J \qquad (4)$$

Where n is the rotational speed in *rev/s* and J is the advanced ratio given by J = $\frac{V_\infty}{nD}$.

The Blade Element Momentum Theory is a combination of the Momentum and Blade Element Theory. The momentum theory assumes the rotor plane to be a sheet with zero thickness which can sustain the pressure difference between the surfaces. The aerodynamic performance of the rotors are calculated based on the induced velocity imparted by the pressure difference. The momentum theory does not take into account the finite number of blades that the rotors have and thus can lead to large prediction errors. The blade element theory on the other hand calculates the rotor properties on each radial section. The blade element momentum theory integrates the finite blade calculations of the blade element theory into the momentum theory to give a better prediction model. All the equations presented below were taken from Matthew et. al [6]. The differential thrust (dT) for each blade section as given by the blade element theory is shown below:

$$dT = \frac{1}{2}\rho V_\infty^2 cB \frac{(1+a_0)^2}{\sin^2 \phi} C_T dr \qquad (5)$$

Where B is the number of blade, a_0 is axial inflow correction factor and ϕ is local inflow angle. The differential torque for each blade section as given by the blade element theory is given by the equation below:

$$dQ = \frac{1}{2}\rho V_\infty cB\omega r^2 \frac{(1+a_0)(1-a_1)}{\sin \phi \cos \phi} C_Q dr \qquad (6)$$

Where r is radial position, ω is rotational velocity in

rad/sec and a_1 is radial inflow correction factor. From equation 5 and 6, C_T and C_Q are related to the local lift and drag coefficients as,

$$\begin{bmatrix} C_T \\ C_Q \end{bmatrix} = \begin{bmatrix} \cos\phi & -\sin\phi \\ \sin\phi & \cos\phi \end{bmatrix} + \begin{bmatrix} C_L \\ C_D \end{bmatrix} \qquad (7)$$

Initialize a_0 and a_1

Calculate C_T and C_Q using initial values of ϕ, angle of attack and Reynolds number (eq-7)

Calculate new values of a_0 and a_1 (eq-10,11)

Calculate new ϕ, angle of attack and Reynolds number from corrected velocities

Replace a_0 and a_1 with new values

Calculate error in inflow correction factors a_0 and a_1

No

Accepted

Yes

Calculate sectional thrust and torque (eq-5,6)

Total Thrust from Numerical Integration

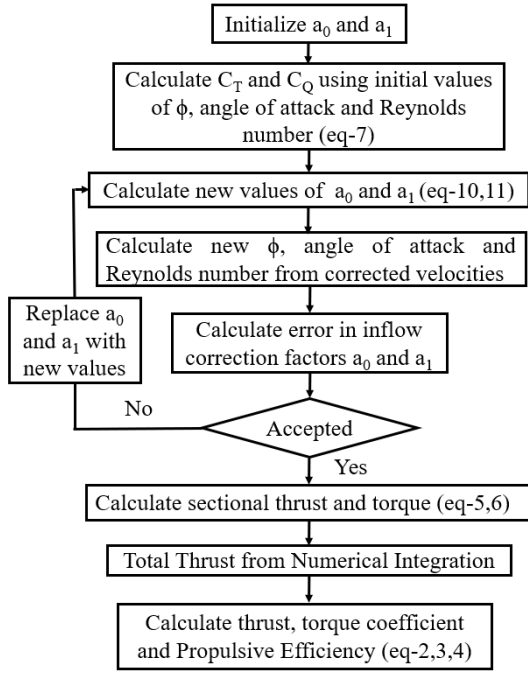Calculate thrust, torque coefficient and Propulsive Efficiency (eq-2,3,4)

Figure 7: BEMT Algorithm Flowchart

The conservation of momentum between the upstream and downstream of propeller gives the differential thrust as

$$dT = 4\pi r \rho V_\infty^2 (1 + a_0) a_0 dr \qquad (8)$$

and the differential torque as

$$dQ = 4\pi r^3 \rho V_\infty (1 + a_0) a_1 dr \qquad (9)$$

From equations 5, 6, 8 and 9 an implicit relationship for induced velocity components are obtained as follow:

$$a_0 = \frac{1}{(4\sin^2\phi/\sigma C_T) - 1} \qquad (10)$$

$$a_1 = \frac{1}{(4\sin\phi\cos\phi/\sigma C_Q) + 1} \qquad (11)$$

Where σ is the local solidity of blade and is given by $cB/2\pi r$. Both radial and axial inflow correction factor

are determined iteratively. Figure 7 illustrates the propeller performance prediction method using BEMT. For more details of the blade element momentum theory, the reader is referred to a textbook by Johnson [11].

3. Results and Discussions

3.1 Validation of BEMT Algorithm

The model of the classical BEMT currently developed was validated by comparing with the full-scale experimental results. The full scale data was extracted from a study carried out by Harrington [12]. Harrington rotor was a two bladed rotor with the diameter of 7.62 m. The rotor solidity was 0.027. The rotors were operating at the tip speed of 152.4 m/s. The blade section used was untwisted with tapered plan form and thickness ratio. NACA four digit symmetric airfoil section was used for the Harrington rotor. The comparison of the resuts from the current BEMT code with the results from the Harrington rotor is shown in Figure 8.
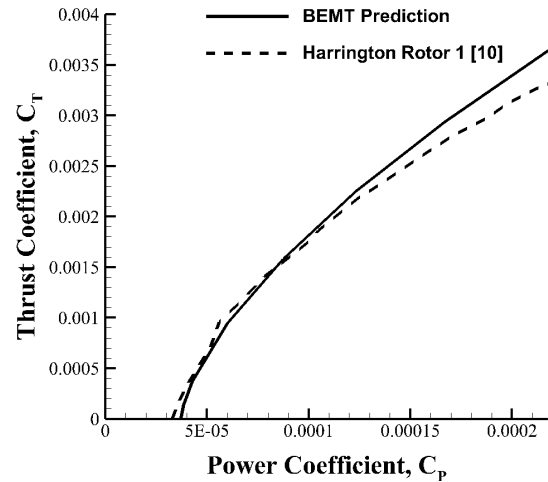
Figure 8: Comparison of Full Scale Tunnel Test Data and BEMT Prediction for Harrington Rotor 1

The plot shows the variation in the thrust coefficient with respect to the coefficient of power. From the figure, it was observed that there was a good agreement between the theoretical and experimental results. The plot shows a good fit until the thrust value of around 0.002. The deviation between the theoretical and experimental results above the thrust coefficient of 0.002 might be due to stall effects. The stalling phenomena in the experimental conditions is

not predicted by the BEMT theory which could be one of the possible explanation for the deviation. The other reason might be due to the underlying assumption of the BEMT itself, i.e., the assumption of small angle of attack. The small angle assumption is violated at higher thrust values which might be the other possible explanation for the observed deviation.

Besides the small angle assumption, inviscid flow and thin airfoil are other underlying assumptions in the classical BEMT. The inviscid assumption is valid for full-scale operations where the Reynolds number are in the order of millions. At high Reynolds number, the inertial effects are more dominant compared to the viscous effects. Thus, the classical BEMT is adequate for predicting the performance of the full scale rotors. But for the low Reynolds number case, the classical BEMT fails to produce reliable results. Thus, modifications in the classical BEMT has been done to include the effects of large angles of attack and viscosity. The database from the XFOIL software has been used to include these effects and the results from the modified BEMT has been discussed in the next sections.

3.2 Effects of Rotational Speed

After the modifications were made to the classical BEMT model, the results from the model were analysed at different operating conditions. The rotational speed of propeller was varied from 6700 RPM to 8500 RPM with freestream velocity varied as 70 m/s, 80 m/s and 90 m/s. The variation of thrust coefficient, torque coefficient and propulsive efficiency with respect to the rotational speed of the propeller has been discussed in this section.

Figure 9 shows the variation of thrust coefficient with respect to rotational speed for different free stream velocities. From the figure, it can be seen that the thrust coefficient of the rotors increased with increasing rotational speed for a constant freestream velocity. The increased thrust is due to the increase in tangential velocity component in the velocity triangle (u_T) as shown in figure 1. The increase in the u_T increases the effective angle of attack in the velocity triangle which consequently increases the thrust produced by the rotors. Following this argument, for the same rotational speed, the thrust should decrease with increasing the freestream velocity due to increase in induced velocity component (u_p). The increase in the induced velocity reduces the effective angle of attack and thus, reducing the thrust value. The current

argument is confirmed by the figure where the minimum thrust is observed for the case of maximum freestream velocity.

The variation in the torque produced by the rotors with respect to the rotational speed at different freestream velocity is shown in figure 10. For larger freestream velocities, increasing trend in the torque with increasing rotational speed was observed. However, the change in the torque was observed to be insignificant for smaller freestream velocity of 70 m/s. Such differences in torque variation can be explained by the changes in thrust coefficient as observed in figure 9. The aerodynamic torque produced by the rotors are directly proportional to the thrust as shown by equation 9. The percentage increase in the propeller thrust for freestream velocity of 80 m/s and 90 m/s (figure 9) was approximately 40% and 85% respectively. This is much higher than the net increase in the thrust for freestream velocity of 70 m/s which was observed to be around 27%. Following this argument, the increase in torque for lower freestream velocities should be small which is confirmed by the figure 10.
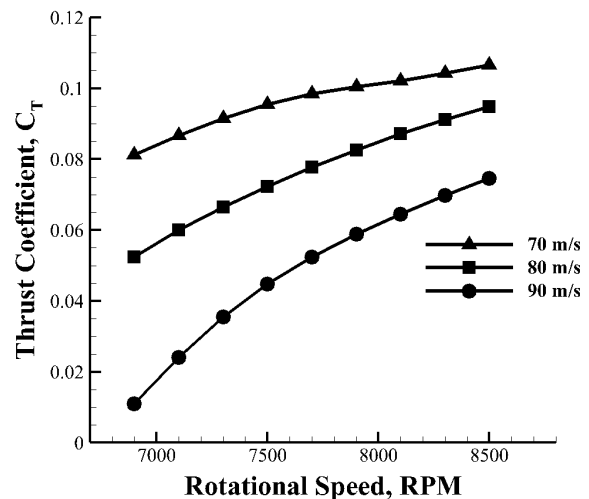
Figure 9: Variation of Thrust Coefficient with Rotational Speed

Furthermore, it can also be observed that the net increase in the torque is not equal to the net increase in thrust because the torque is dependent on other factors such as the correction factor which is shown in equation 9. In figure 10, it was also observed that the torque required by the propeller at the freestream velocity of 90 m/s was minimum compared to the cases of lower freestream velocity. Propellers require lower power to produce the same thrust at higher
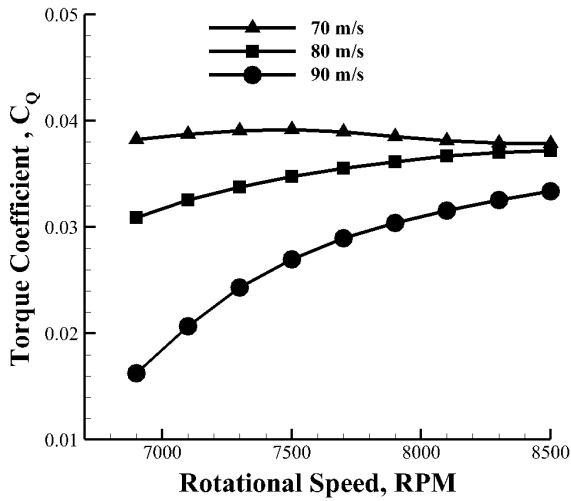
Figure 10: Variation of Torque Coefficient with Rotational Speed

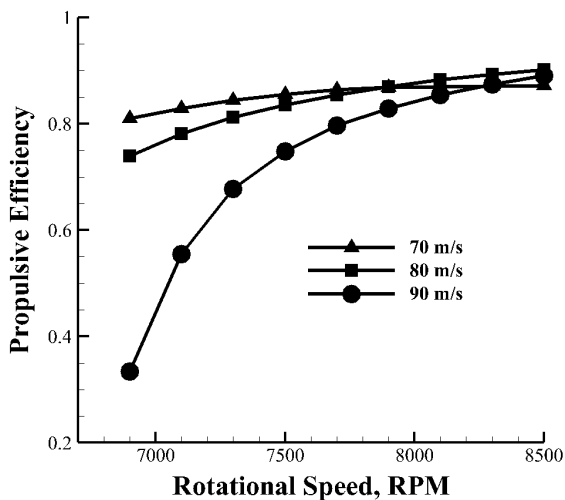induced velocities which is in part with the current observation.

Figure 11: Variation of Propulsive Efficiency with Rotational Speed

The variation in the propulsive efficiency with respect to the rotational speed is shown in figure 11. The figure shows that for free stream velocity of 70 m/s, propulsive efficiency first increases, reaches to its maximum value of 0.87 at 7897 RPM and starts to decrease. For other forward speeds, propulsive efficiency increases with rotational speed within our operational bound. For design point the propulsive efficiency was found to be 0.835. From the figure, it was also observed that the efficiency of the propeller

was quite low at smaller rotational speeds when the freestream velocity was set at 90m/s. The current observation suggests that the propeller should not be operated at lower RPMs when the freestream velocity are large.

3.3 Effects of Freestream Velocity

The freestream velocity of propeller was varied from 67 m/s to 85 m/s. For three rotational speed 7000 RPM, 7500 RPM and 8000 RPM, the variation of thrust coefficient, torque coefficient and propulsive efficiency with respect to the freestream velocity is studied in this section.
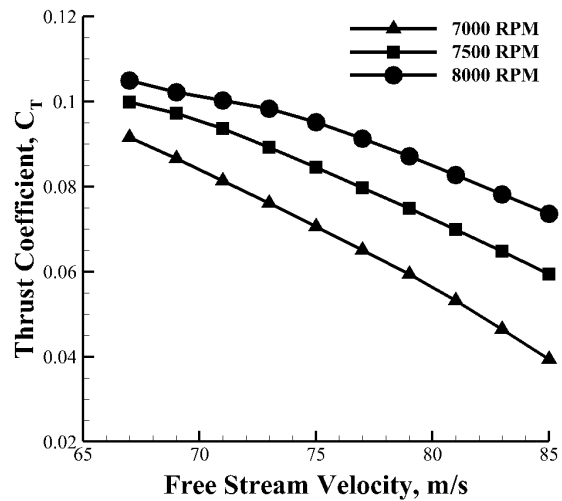

Figure 12: Variation of Thrust Coefficient with Free Stream Velocity

Figure 12 shows the plot between freestream velocity and thrust coefficient. The thrust was observed to reduce with increasing freestream velocity. The thrust was also observed to be smallest for the lower rotational speed of 7000 RPM. From plot it was observed that the difference between thrust coefficient for different rotational speed increases with increasing forward speed. At design point the thrust coefficient value was found to be 0.0724. The observations currently made is in part with the theory as explained in the earlier section. The current plot serves as a selection tool for the vehicle design to get an estimate of the propeller performance at different operating conditions.

In figure 13 variation of torque coefficient with free stream velocity was plotted. Which shows that the value of torque coefficient is decreasing with increasing value of free stream velocity for all
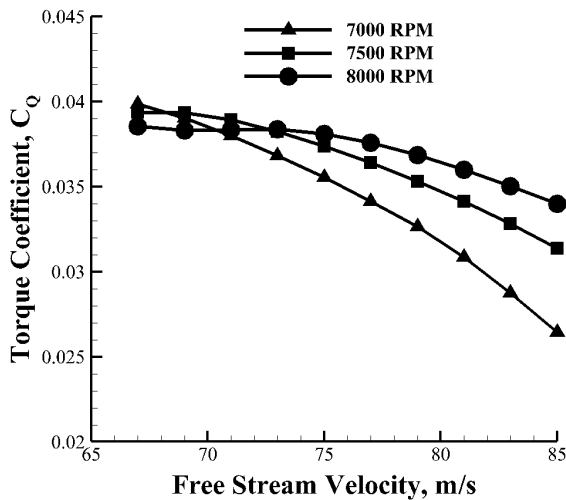
Figure 13: Variation of Torque Coefficient with Free Stream Velocity

rotational speeds. The current observation is expected as the thrust is also reducing with increasing freestream velocity. The aerodynamic torque is directly correlated with the thrust which explains the reduction in the torque coefficient. For design point the torque coefficient value was 0.0347.
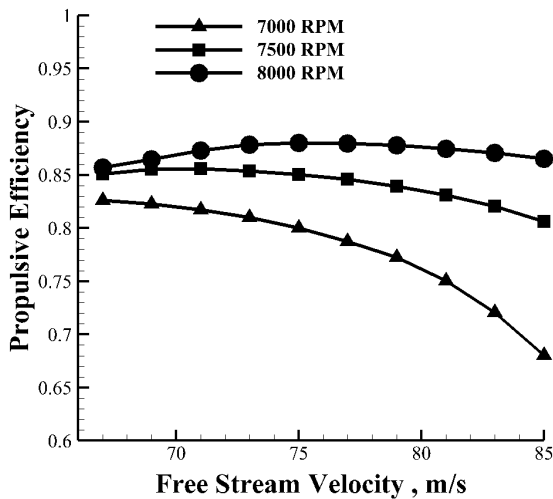

Figure 14: Variation of Propulsive Efficiency with Free Stream Velocity

Variation of propulsive efficiency against free stream velocity was plotted in Figure 14 for different value of rotational speed. The figure shows that for RPM of 8000, the efficiency first increased, reached its maximum value and started to decrease. But for other RPMs, the efficiency was observed to decrease with increasing freestream velocity. The change in the

propulsive efficiency with respect to the freestream velocity was observed to be minimum when compared to its change with respect to the rotational speed. At design point the propulsive efficiency was observed to be 0.835. The current phenomena is again in part with the theoretical explanation as presented in the earlier section.

The observations made in the current paper shows that the modified BEMT currently developed seems to capture the physical trends which is in part with the existing theory. The results presented so far suggests that the current tool can be used to understand the general behaviour of the propeller at different on design operating conditions. But the quantitative efficacy of the current model still needs to be validated. Thus, the comparison of the current model with the experimental results will be carried out in the future.

4. Conclusions

Availability of propeller performance data for the design point and off design points helps UAVs designer to select the suitable propeller for the specific operating conditions. After validation of MATLAB codes written for the classical BEMT, performance analysis of the designed propeller at different design conditions was carried out. Some of the conclusions that can be made from the current study are listed below:

1. The thrust and torque of the propeller was observed to increase with increasing the rotational speed for all freestream velocities. The thrust produced was minimum for larger freestream velocity of $90m/s$.

2. The change in the torque with respect to the rotational speed was observed to be small for freestream velocity of $70m/s$ when compared to the larger velocities.

3. The efficiency of the propeller was observed to be low for smaller rotational speeds when the freestream velocity was $90m/s$.

4. The propeller thrust and torque was observed to decrease with increasing freestream velocity for all rotational speed.

5. The changes in the propulsion efficiency with respect to the freestream velocity was observed to be less significant.

6. At design point, the thrust coefficient, torque coefficient and propulsive efficiency were found to be 0.0724, 0.0347 and 83.5 respectively

5. Future Works

1. The validation of developed tool will be done by predicting the performance of APC 10x7 propeller for which propeller geometry, operating conditions and database will be taken from Matthew et. al [6].

2. The results from the current tool will be validated with the existing experimental results for both the twisted and untwisted bladed rotors.

3. The output from prediction tool will be compared with computational fluid dynamics (CFD) analysis and experimental results. The structural analysis of propeller will also be performed.

4. Finally, an experimental setup will be developed for further validation of the current tool.

6. Recommendations

This research work is limited to the performance prediction of propeller with in a certain operational bound because of the unavailability of post stall data for BEMT algorithm. Aerodynamic database can be extended to post stall regions in both directions and performance prediction of propeller can be done in all possible operational range.

Acknowledgments

References

[1] Saleen Bhattarai, Kushal Poudel, Nishant Bhatta, Sanjay Mahat, Sudip Bhattarai, and Kaman S Thapa Magar. Modeling and development of baseline guidance navigation and control system for medical delivery uav. In *2018 AIAA Information Systems-AIAA Infotech@ Aerospace*, page 0508. 2018.

[2] David Wall. *Optimum propeller design for electric UAVs*. PhD thesis, 2012.

[3] Monal Merchant and L Scott Miller. Propeller performance measurement for low reynolds number uav applications. In *44th AIAA aerospace sciences meeting and exhibit*, page 1127, 2006.

[4] John Brandt and Michael Selig. Propeller performance data at low reynolds numbers. In *49th AIAA Aerospace Sciences Meeting including the New Horizons Forum and Aerospace Exposition*, page 1255, 2011.

[5] Donghun Park, Yunggyo Lee, Taehwan Cho, and Cheolwan Kim. Design and performance evaluation of propeller for solar-powered high-altitude long-endurance unmanned aerial vehicle. *International Journal of Aerospace Engineering*, 2018, 2018.

[6] Matthew H McCrink and James W Gregory. Blade element momentum modeling of low-reynolds electric propulsion systems. *Journal of Aircraft*, pages 163–176, 2017.

[7] Onur Günel, Emre Koç, and Tahir Yavuz. Cfd vs. xfoil of airfoil analysis at low reynolds numbers. In *2016 IEEE International Conference on Renewable Energy Research and Applications (ICRERA)*, pages 628–632. IEEE, 2016.

[8] Lance W Traub and Evan Cooper. Experimental investigation of pressure measurement and airfoil characteristics at low reynolds numbers. *Journal of aircraft*, 45(4):1322–1333, 2008.

[9] Norman Sissenwine, Maurice Dubin, and Harry Wexler. The us standard atmosphere, 1962. *Journal of Geophysical Research*, 67(9):3627–3630, 1962.

[10] Xinqiang Liu and Weiliang He. Performance calculation and design of stratospheric propeller. *IEEE Access*, 5:14358–14368, 2017.

[11] Wayne Johnson. *Rotorcraft aeromechanics*, volume 36. Cambridge University Press, 2013.

[12] Robert D Harrington. Full-scale-tunnel investigation of the static-thrust performance of a coaxial helicopter rotor. 1951.